Temperature Dependence of Segmental Mobility in Poly(ethylene oxide) Complexed with $Ba(ClO_4)_2$: A Carbon-13 NMR Study

Staffan Schantz*

Department of Polymer Technology, Chalmers University of Technology, S-41296 Göteborg, Sweden

Sirkka L. Maunu

Department of Polymer Chemistry, University of Helsinki, PB 13, FIN-00014 HY, Helsinki, Finland

Received June 1, 1994; Revised Manuscript Received August 1, 1994®

ABSTRACT: The local polymer chain mobility of low molecular weight poly(ethylene oxide) (PEO) complexed with $Ba(ClO_4)_2$ has been investigated with ^{13}C NMR techniques over the temperature range 297–463 K. The carbon line width and the rotating frame spin–lattice relaxation rate provide information of segmental motion in the mid-kilohertz region, as shown by their temperature dependencies with clear maxima at ~327 K. The laboratory frame spin–lattice relaxation rate maximum is observed at ~378 K, consistent with the progressive changes in correlation times of motion above the glass transition temperature. When comparing the present relaxation data for PEO–$Ba(ClO_4)_2$ with those from the literature for PEO, we find that salt complexation dramatically slows down the segmental motions in the amorphous phase. The average correlation time curve of the PEO–salt complex is shifted to higher temperatures and shows greater temperature sensitivity in comparison with PEO.

Introduction

Solid polymer electrolytes are interesting materials due to their relatively high ionic conductivity (at best on the order of ~10^{-3} S/cm) combined with the favorable mechanical properties normally associated with polymeric materials. This field of research has been very active since Armand first suggested that poly(ethylene oxide) (PEO) based salt complexes can be used in various electrochemical devices.[1] Examples of possible applications are rechargeable solid-state batteries, fuel cells, and sensors.[2]

It is generally agreed that the ionic conductivity in polyether–salt complexes is related to the segmental mobility of the polymer molecules.[3,4] High chain mobility above the glass transition temperature (T_g) is a requirement for fast ion diffusion. Unfortunately, the viscosity increases dramatically by salt complexing the polymer. The rise in viscosity has been attributed to the solvation of the salt; the cations are thought to act as transient cross-links between the ether oxygens of adjacent chains. This will reduce the flexibility of the system, as is also demonstrated by the increasing values of T_g with salt concentration, and may therefore decrease the ionic mobility. Plots of conductivity vs salt concentration typically show a maximum at high salt concentrations (around an oxygen to salt ratio O:M ~ 10 for monovalent salts), which is thought to result mainly from a reduced ionic mobility.[3,4] It is the *local* chain mobility that is believed to assist the migration of ions, i.e., the reorientation of a few polymer segments.

The knowledge about chain mobility in polymer electrolytes is limited. Traditional dynamic methods such as NMR and dielectric spectroscopy techniques have mainly been used in studies of ion diffusion in various polymer–salt complexes.[5–8] Torell and co-workers have used inelastic light scattering to investigate both chain motion and ion association effects in poly(propylene oxide) (PPO) salt-complexed systems.[9–13] It was found by high-frequency Brillouin scattering that the chain motion slows down considerably as the salt concentration increases. Raman scattering data proved the existence of significant ion–ion interactions. Ion pairing was however found to have only a minor influence on the conductivity. Recent investigations of PPO–$NaCF_3SO_3$ by the same group indicate the presence of two relaxation processes revealed at the low frequencies (~Hz to kHz) probed in photon correlation spectroscopy.[13] Both processes were attributed to segmental motions: the slower relaxation to segments that are transiently cross-linked by the solvated ions and the faster process to motions of more mobile segments away from the cross-links. Other reports of unusually broad or even split glass transitions support the view of heterogeneity in these systems.[8,14] PEO–salt systems may, in addition to various local structures in the amorphous phase, contain crystalline regions. Thus, the multiphase character of polymer electrolytes emphasizes the need for selective characterization techniques.

NMR has long been employed in observing molecular motion and has been extensively applied to the complex problems presented by macromolecules. Due to the short range nature of the technique it is suitable for investigations of local mobility. However, in the field of polymer electrolyte dynamics only a few NMR studies have been reported up to now.[15–17] In the present work we have used ^{13}C NMR to study the chain mobility in PEO–$Ba(ClO_4)_2$ of salt concentration O:M = 10. Various relaxation times obtained as a function of temperature allow us to cover a relatively broad time window, i.e. molecular motions with correlation times ~10^{-5}–10^{-9} s.

^{13}C NMR Background

In ^{13}C NMR of solids relatively narrow line widths can be obtained by using magic angle spinning (MAS) combined with broad-band proton decoupling (DD). MAS of the sample averages the chemical shift to its isotropic value, and proton radio-frequency irradiation modulates the dipolar interaction of the protons with the carbon-13 nuclei. The remaining line width, $1/(\pi T^*_2)$, can be expressed as[18]

® Abstract published in *Advance ACS Abstracts*, September 15, 1994.

0024-9297/94/2227-6915$04.50/0

$$\frac{1}{\pi T^*_2} = \frac{1}{\pi T_{2o}} + \frac{1}{\pi T_{2c}} + \frac{1}{\pi T_{2m}} \quad (1)$$

where the first term is the intrinsic line width due to static contributions, such as missetting of the magic angle and magnetic susceptility broadening, and the second term represents variations in molecular packing and conformational inequivalence. The third term describes dynamic ("homogeneous") broadening which may be observed when molecular motions produce magnetic fields fluctuating at frequencies close to the MAS angular frequency and/or the angular frequency of the proton decoupling field, ω_{1H}. As a consequence, the modulation of chemical shift anisotropy (MAS) and/or dipolar interaction (DD) is diminished and the NMR resonance broadens.[18,19] Thus, MAS/DD line width experiments may probe molecular motions with correlation times typically in the range $\sim 10^{-5}$–10^{-6} s.

^{13}C NMR relaxation in the rotating frame, $T_{1\rho}(C)$, is another probe of kilohertz mobility. Both spin–lattice (motional) and spin–spin (nonmotional) processes may contribute to the observed relaxation according to[20,21]

$$\frac{1}{T_{1\rho}} = \frac{1}{T_{1\rho}^{\text{spin-lattice}}} + \frac{1}{T_{1\rho}^{\text{spin-spin}}} \quad (2)$$

$T_{1\rho}^{\text{spin-lattice}}$ is due to motional modulation of the ^{13}C—^{1}H internuclear dipolar interactions at the rotating frame Larmor frequency ($\omega_{1C}/(2\pi) = 42$ kHz in the present study), and $T_{1\rho}^{\text{spin-spin}}$ involves mutual spin flip–flops of ^{13}C—^{1}H pairs. In the case of a predominantly motional relaxation pathway $1/T_{1\rho}(C)$ is at maximum when the rate of molecular motion is close to ω_{1C}.

Mobility in the megahertz region provides a strong effect on the ^{13}C spin–lattice relaxation in the laboratory frame, $T_1(C)$. Assuming a ^{13}C—^{1}H dipolar relaxation mechanism only we have[22]

$$\frac{1}{T_1(C)} = \frac{N}{10}\left(\frac{\mu_0 \gamma_H \gamma_C \hbar}{4\pi r^3}\right)^2 [J(\omega_H - \omega_C) + 3J(\omega_C) + 6J(\omega_H + \omega_C)] \quad (3)$$

where N is the number of directly bonded protons, μ_0 is the vacuum magnetic permeability, γ_C and γ_H are the magnetogyric ratios of ^{13}C and ^{1}H nuclei, respectively, r is the C—H internuclear distance, $J(\omega)$ is the spectral density of motion, and ω_C and ω_H are the ^{13}C and ^{1}H Larmor frequencies, respectively. For a quantitative evaluation of data the crucial point is the choice of $J(\omega)$, which is a complex problem for polymer chain motion. For isotropic motion with a single correlation time, τ, the spectral density is given by

$$J(\omega) = \frac{\tau}{1 + \omega^2\tau^2} \quad (4)$$

Motion of a polymer chain is however far from isotropic, as is well documented in the literature.[23,24] There may also be a distribution of exponential correlation times arising from the local structural heterogeneity characteristic of a glass.[21,23] Therefore, phenomenological distribution functions are often used in fitting relaxation data. The Havriliak–Negami (HN) function is one example which originates from the interpretation of dielectric relaxation experiments.[25] The HN asymmetric spectral density for NMR relaxation is given by[26]

$$J(\omega) = \frac{1}{\omega}\sin\left[\epsilon \arctan\left\{\frac{(\omega\tau)^\delta \sin(\delta\pi/2)}{1 + (\omega\tau)^\delta \cos(\delta\pi/2)}\right\}\right][1 + 2(\omega\tau)^\delta \cos(\delta\pi/2) + (\omega\tau)^{2\delta}]^{-\epsilon/2} \quad (5)$$

where the parameters fulfill $0 < \delta < 1$ and $\epsilon < \delta^{-1}$. Equation 5 reduces to a symmetric distribution (Cole–Cole) when $\epsilon = 1$ and to the isotropic spectral density (eq 4) when $\epsilon = \delta = 1$. The HN distribution has properties similar to the spectral density obtained from the nonexponential Kolrausch–Williams–Watts (KWW) correlation function.[26]

Experimental Section

Materials. Low molecular weight PEO (from Fluka) was used as the host polymer. The weight- and number-average molecular weights were determined by gel permeation chromatography (GPC): $M_w = 7100$ and $M_n = 5800$, respectively. The melting temperature was ~338 K and the degree of crystallinity was about 90%, as calculated from the melting enthalpy.

Preparation of the PEO–$Ba(ClO_4)_2$ complex is described in detail in ref 27. The anhydrous salt (purity >98% from Fluka) was dissolved in the polymer with the monomer to salt ratio O:M = 10 using methanol. The solvent was then evaporated and the sample dried at 353 K for several days. After this procedure the content of water and low molecular weight residues in the sample amounted to less than 0.5% by weight, as determined by thermogravimetry and FTIR. Between and during measurements the sample was kept in a dry atmosphere. The degree of crystallinity of the complex was less than 15%, as calculated using the melting enthalpy value of uncomplexed PEO. This number is probably an overestimation of the upper limit, because no signs of crystallinity were detected in previous proton[27] or present carbon NMR measurements. The melting temperature of the crystalline phase was ~393 K. The glass transition temperature of the sample was found to be approximately 316 K using standard DSC conditions.

NMR Methods. Experiments were performed on a Varian VXR300 spectrometer, operating at 75.4 and 299.9 MHz for ^{13}C and ^{1}H, respectively. The sample was packed as a powder in a silicon nitride rotor with a torlon endcap and spun at 4 kHz (±10 Hz) in a Varian variable temperature CPMAS probe in most of the experiments. The sample was allowed to equilibrate for at least 20 min at each temperature before starting the measurement. Following Haw et al. the sample temperature was calibrated using samarium acetate tetrahydrate as a chemical shift thermometer and the solid–solid phase transitions of 1,4-diazabicyclo[2.2.2]-octane and *d*-camphor as temperature markers.[28,29]

Direct-polarization MAS/DD spectra were obtained following a single ^{13}C $\pi/2$ pulse and with a proton decoupling field strength $\omega_{1H}/(2\pi) \sim 70$ kHz. Rotating frame relaxation times, $T_{1\rho}(C)$, were determined by varying the carbon spin-lock time after cross-polarization (CP) between protons and carbons.[21] The carbon rf field strength was $\omega_{1C}/(2\pi) = 42$ kHz. Torchia's method[30] (with CP) and a direct inversion-recovery sequence (without CP) were used to measure laboratory frame carbon spin–lattice relaxation times, $T_1(C)$. Proton saturation with a low-level field during the recovery of the carbon spins did not cause any detectable change in these measurements; all T_1 decays/recoveries were found to be single exponential. At temperatures above ~380 K the $T_1(C)$ measurements were performed using a standard broad-band probe with slow sample spinning and low-power proton decoupling ($\omega_{1H}/(2\pi) = 2.5$ kHz).

Results and Discussion

Carbon NMR Line Shapes. Many solid-state NMR studies of PEO appear in the literature, and it is well established that the carbon-13 line shape consists of two components corresponding to crystalline and amorphous regions, respectively.[18,31,32] At room temperature the crystalline component at ~72 ppm dominates the band envelope due to homogeneous broadening.[18,31] The amorphous peak is much narrower and shifted upfield ~1 ppm.

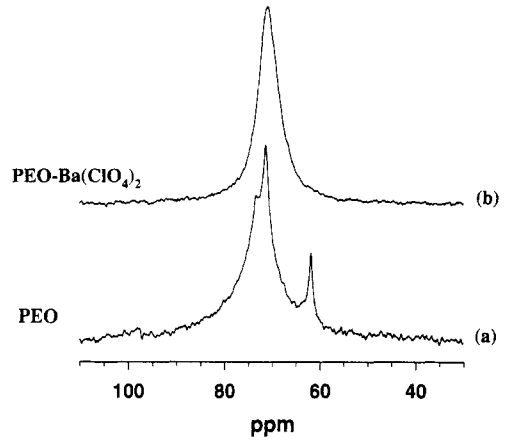

Figure 1. ^{13}C MAS/DD NMR spectra of PEO (a) and PEO–$Ba(ClO_4)_2$ (b), using a recycle time of 0.64 s (a) and 3 s (b).

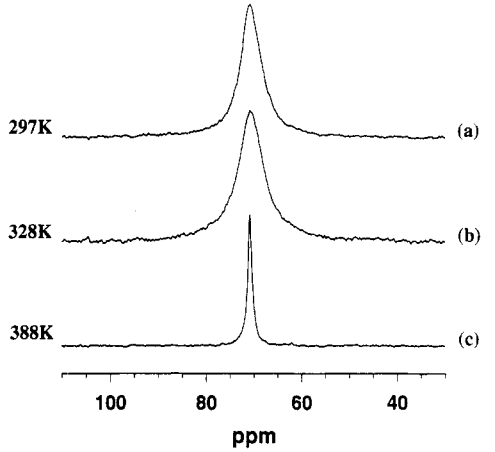

Figure 2. ^{13}C MAS/DD NMR spectra of PEO–$Ba(ClO_4)_2$ at 297 K (a), 328 (b), and 388 K (c).

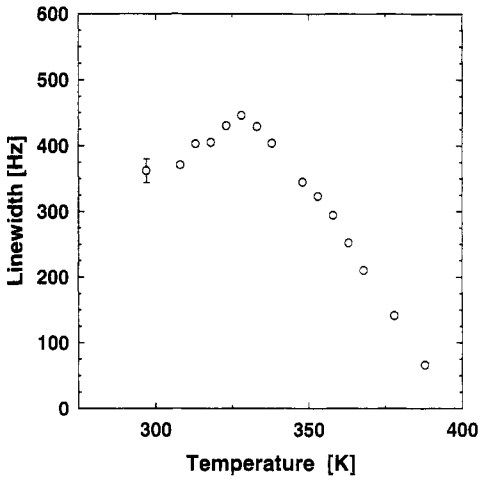

Figure 3. Temperature dependence of the carbon-13 MAS/DD line width of PEO–$Ba(ClO_4)_2$.

In Figure 1a is shown the ^{13}C MAS/DD spectrum of the low molecular weight PEO (M_n = 5800) used in the present study. In addition to the two components at ~71 and ~72 reported for high molecular weight PEO, a third peak appears at 61 ppm which is due to the chain end group, $\sim CH_2OH$.[33] Note that the intensities of PEO in Figure 1a are not representative of a respective carbon site; a short recycle time of 0.65 s between pulses was used in order to suppress the crystalline component (~90% DSC crystallinity) which has a spin–lattice relaxation time (T_1(C)) of several seconds at room temperature. T_1(C) for the amorphous main-chain peak and the end group are both shorter than ~1 s, which exaggerates their intensities in Figure 1a. The end group resonance has contributions from molecules in both crystalline and amorphous regions, which explains why its intensity is comparable to the amorphous main-chain resonance in Figure 1a. The equilibrium spectrum taken above the melting temperature gives intensities for the 71 and 61 ppm resonances in accordance with the end group concentration from GPC measurements.

From Figure 1b it is obvious that the addition of salt to PEO causes a significant broadening of the amorphous ^{13}C resonance (Figure 1b is the equilibrium spectrum of PEO–$Ba(ClO_4)_2$, obtained using a long recycle time). At 297 K the half-width is ~360 Hz for the PEO–$Ba(ClO_4)_2$ complex compared to less than 100 Hz for amorphous PEO. It is known from previous investigations that PEO–$Ba(ClO_4)_2$ of composition O:M = 10 is predominantly amorphous.[34] This is consistent with the observed chemical shift which is the same for the amorphous peak of PEO and PEO–$Ba(ClO_4)_2$ (Figure 1). Furthermore, recent proton rotating frame relaxation[27] and the present carbon T_1 data (see below) are best fitted to single exponential relaxations, which is in agreement with a very low degree of crystallinity. It is probable that some of the line broadening upon salt complexation is due to local structural heterogeneity; i.e. it could partly be due to a distribution of carbon sites with different ion–polymer interactions. The measured line widths were however found to be the same (within the experimental accuracy) in CPMAS/DD and MAS/DD experiments, which indicates that the polymer–salt complex is not highly heterogeneous with a defined multiphase character. This is because cross-polarization accentuates the contribution of the most rigid carbons, whereas direct-polarization experiments with long recycle delays give equilibrium spectra with the same contribution from each carbon-13 spin.

In Figure 2 MAS/DD spectra of the PEO–salt complex are shown at some selected temperatures. The temperature dependence reveals that also motional processes contribute strongly to the line width. Increasing the temperature from 297 to 328 K results in a ~20% increase of the ^{13}C line width to ~450 Hz. For even higher temperatures the peak gradually narrows; the half-width is only ~70 Hz at 388 K. In Figure 3 the line width is plotted vs temperature from slightly below T_g to ~T_g + 70 K. The behavior reflects a typical temperature dependence expected for homogeneous broadening (see eq 1). At temperatures around the calorimetric glass transition proton decoupling is relatively efficient in averaging the dipolar carbon–proton coupling, whereas above ~330 K the line width is decreased by rapid motional averaging. The maximum in Figure 3 reflects the matching between the rate of chain motion and the precession angular frequency about the proton decoupling field (ω_{1H}). This gives, with $\omega_{1H}/(2\pi)$ = 70 kHz, an average correlation time $\langle\tau\rangle = 2.3 \times 10^{-6}$ s at ~328 K. The crystalline phase of uncomplexed PEO is reported to show behavior similar to that of amorphous PEO–$Ba(ClO_4)_2$ of the present study.[18,31] In fact, the large line width of the crystalline ^{13}C PEO peak at room temperature has been shown to result from the same mechanism as discussed here; see Figure 1a.[18,31] This implies a very low chain mobility for the amorphous salt-complexed system with motional correlation times comparable to those of crystalline PEO at around room temperature.

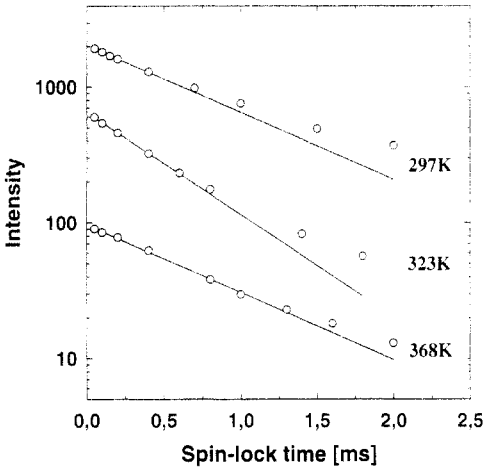

Figure 4. Representative carbon-13 $T_{1\rho}$(C) data of PEO–$Ba(ClO_4)_2$ at some temperatures. $\langle T_{1\rho}(C)\rangle$ is taken from the initial part of the curves (straight lines).

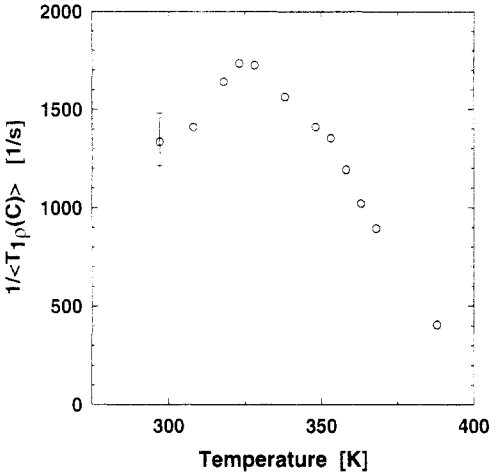

Figure 5. Temperature dependence of $1/\langle T_{1\rho}(C)\rangle$ for PEO–$Ba(ClO_4)_2$. $\langle T_{1\rho}(C)\rangle$ is taken as in Figure 4.

The line width was found to be very sensitive to the decoupling field strength at temperatures below the maximum. Decreasing $\omega_{1H}/(2\pi)$ from 70 to 36 kHz at 297 K broadens the resonance from ~360 to ~680 Hz. On the other hand, at higher temperatures well above the maximum in Figure 3 the line width is insensitive to the decoupling power. At 378 K, line widths as obtained with MAS/DD agree within ±10% with those obtained with low-power decoupling; i.e. a change in $\omega_{1H}/(2\pi)$ from 2.5 to ~70 kHz does not significantly affect the line width in this temperature region. These results of the field strength dependence are in accordance with a carbon-13 resonance homogeneously broadened by modulation of $^{13}C—^{1}H$ dipolar interactions. We then expect a strong field dependence in the slow motion regime ($1/T_{2m} \sim 1/(\omega_{1H})^2$ for isotropic motion) and a weak field dependence in the fast motion regime ($1/T_{2m}$ is independent of ω_{1H} for isotropic motion).[18,19]

Another possible motional broadening mechanism in ^{13}C MAS/DD experiments is the motional modulation of chemical shift anisotropy.[18,35] A maximum in line width may then be observed when the molecular correlation times are on the order of the inverse MAS angular frequency. For such a process one would expect a strong line width dependence on the MAS frequency in the slow correlation time regime ($1/T_{2m} \sim 1/(\omega_{MAS})^2$ for $\omega_{MAS}\tau \gg 1$ and isotropic motion). However, at room temperature the half-width was found to decrease only by ~30 Hz when increasing the MAS frequency from 2 to 6 kHz, which excludes modulation of chemical shift anisotropy as the broadening mechanism for PEO–$Ba(ClO_4)_2$ in the temperature region investigated.

Carbon $T_{1\rho}$(C) Relaxation. Results of $T_{1\rho}$(C) measurements at some temperatures are shown in Figure 4. The carbon magnetization decay is clearly deviating from a single-exponential process. Dispersions similar to those in Figure 4 were found throughout the temperature range investigated. Nonexponential $T_{1\rho}$(C) relaxation for polymers is a common finding, in contrast to proton spin–lattice relaxation which is often averaged by spin diffusion to give a single-exponential relaxation decay. Schaefer et al. investigated a range of glassy polymers and suggested that the observed $T_{1\rho}$(C) dispersions are due to different slowly (on the NMR time scale) interconverting local configurations, each characterized by a single relaxation time, leading to several $T_{1\rho}$(C) relaxation times.[21] It is tempting to assign the dispersions in Figure 4 to the heterogeneous structure of salt-complexed PEO; i.e. the $T_{1\rho}$(C) data may partly reflect a distribution of ion–polymer interactions. We note however that other sources of nonexponential relaxations are possible, such as anisotropic motion which may lead to orientation dependent relaxation.[23]

Following the usual procedure we take the average $\langle T_{1\rho}(C)\rangle$ from the initial slope (between 0.05 and 0.8 ms in the present study); see Figure 4. $1/\langle T_{1\rho}(C)\rangle$ values obtained in this way are plotted vs temperature in Figure 5. The shape of the curve is very similar to that of the line width data in Figure 3 with a maximum at ~326 K. The similarity of the two plots implies that the rotating frame relaxation is dominated by motional spin–lattice processes and that nonmotional (spin–spin) relaxation is of minor importance in the temperature range investigated. This is supported by the dependence of $\langle T_{1\rho}(C)\rangle$ on the carbon spin-lock frequency, ω_{1C}, at 297 K. Increasing $\omega_{1C}/(2\pi)$ by a factor of 2 results in an increase of $\langle T_{1\rho}(C)\rangle$ from ~1.0 to ~2.1 ms (using 3 kHz MAS frequency and peak heights as a measure of carbon intensity). Although only two different fields are included in this comparison due to instrumental limitations, the field dependence is relatively weak, which is consistent with a predominantly motional basis for $\langle T_{1\rho}(C)\rangle$.[21]

At the $1/\langle T_{1\rho}(C)\rangle$ maximum the condition $\omega_{1C} < \tau > \sim 1$ with $\omega_{1C}/(2\pi) = 42$ kHz gives an average correlation time of 3.8×10^{-6} s at ~326 K. This value is close to that obtained from the line width data at about the same temperature (~328 K), which indicates that both experiments probe similar PEO chain motions. Although $T_{1\rho}$(C) and the line width data are sensitive to motions in slightly different frequency ranges (42 and 70 kHz, respectively), the frequency difference corresponds to a temperature shift which is within the experimental accuracy.

Our experimental findings of mobility in the midkilohertz region are similar to results recently reported in ref 16, where a value of $\tau = 4.3 \times 10^{-6}$ s was obtained for divalent PEO–triflate complexes of salt concentrations O:M = 9–24 in the temperature region 305–325 K. Proton rotating frame relaxation was used in this study, and the data were analyzed using the isotropic model over a broad temperature range. We have made no attempts to analyze the carbon rotating frame relaxation and line width data of the present study in terms of spectral densities, due to possible spin–spin contributions ($T_{1\rho}$(C)) and static contributions (line width), respectively.

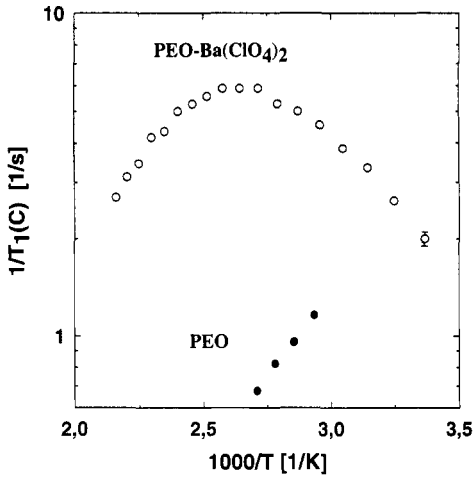

Figure 6. Plot of $1/T_1(C)$ vs inverse temperature for PEO–$Ba(ClO_4)_2$ (○) and PEO (●).

Carbon T_1(C) Relaxation. Results of laboratory frame spin–lattice relaxation time measurements of PEO–$Ba(ClO_4)_2$ are presented in Figure 6. The $T_1(C)$ decays (recoveries) are well described by single-exponential functions over the whole temperature region investigated which, together with the fact that no discontinuity of the relaxation data is seen at the melting temperature of the crystalline phase (~393 K), is consistent with a very low degree of crystallinity. The data taken at temperatures above ~390 K were obtained using standard liquid NMR conditions, i.e. slow sample spinning and low-power proton decoupling. The line-narrowing technique (DD) is not necessary at these temperatures because of the high chain mobility which modulates the $^{13}C—^{1}H$ dipolar coupling and thereby reduces the line width.

The plot of $1/T_1(C)$ vs inverse temperature in Figure 6 shows an asymmetric curve with a broad maximum at ~378 K, which gives an average correlation time $\langle\tau\rangle \sim 1/\omega = 2.1 \times 10^{-9}$ s. The temperature of the $1/T_1(C)$ maximum is ~50 K above the rotating frame/line width maxima (Figures 3 and 5) and approximately 60 K above the DSC glass transition temperature. These observations are consistent with the fact that the different carbon relaxations are sensitive to molecular mobility in different frequency regions, and they suggest that the observed motions belong to the glass transition phenomena. Such motions are characterized by very broad distributions of correlation times, especially for polymers. Indeed, the isotropic model with a single correlation time cannot explain the $1/T(C)$ data in Figure 6. From eqs 3 and 4, we calculate $1/T_1(C) = 17$ s^{-1} at the relaxation rate maximum. This value is much higher than the experimentally obtained 6 s^{-1}. Furthermore, the broad and asymmetric shape of the relaxation maximum is not consistent with isotropic motion. Although phenomenological distribution functions, such as the Havriliak–Negami spectral density (eq 5), can fit the relaxation data of PEO–$Ba(ClO_4)_2$ in Figure 6, the obtained temperature dependence for τ was found to be inconsistent with the midkilohertz carbon relaxation data. For example, by assuming an Arrhenius temperature dependence for τ in this temperature region, we obtain an apparent activation energy of 150 kJ/mol as calculated by combining $\langle\tau\rangle$ from the $1/T_{1\rho}(C)$ and the $1/T_1(C)$ maxima, respectively. However, from the best fit of the $1/T_1(C)$ data using the Havriliak–Negami spectral density (with $\epsilon = 0.73$ and $\delta = 0.40$ in eq 5), we calculate a much lower activation energy of 78 kJ/mol. The agreement is not improved much by assuming an approximate free volume dependence for τ over the temperature region investigated. An explanation for the discrepancy may be that the width of the correlation time distribution is temperature dependent. We have made no further attempt to interpret the $T_1(C)$ data.

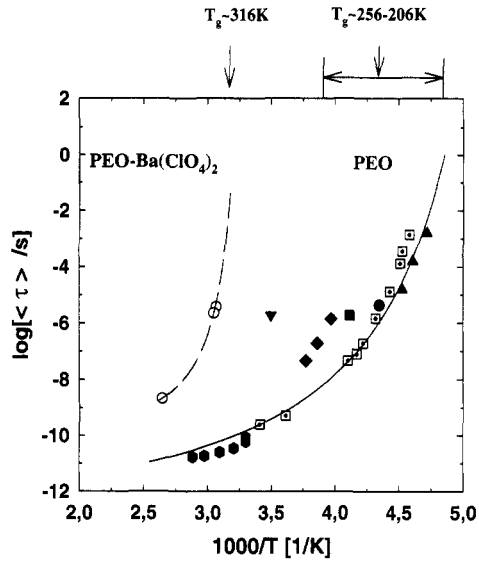

Figure 7. Arrhenius plot of the average correlation time for PEO–$Ba(ClO_4)_2$ of salt concentration O:M = 10 and for PEO. Open circles correspond to the carbon-13 relaxation rate maxima in Figures 3, 5, and 6 for PEO–$Ba(ClO_4)_2$. The dashed line is a guide to the eye. Proton NMR relaxation data are for PEO of molecular weights 4×10^6 (●),[31] 3×10^4 (■), and 5×10^3 (▼).[37] Dielectric relaxation data are for PEO of molecular weights 5×10^6 (▲),[38] 2.8×10^6 (⊡),[40] and 3×10^4 (⬢)[39] (◆).[40] The solid curve is from a WLF fit of carbon relaxation data for PEO.[36] The glass transition temperature of PEO–$Ba(ClO_4)_2$ and the T_g range for PEO of various molecular weights are included.[41]

Comparisons with Uncomplexed PEO. The fraction of amorphous material is unfortunately low for the PEO sample used (~10%), and it is therefore cumbersome to obtain carbon relaxation data for comparisons with the PEO–salt complex. We have instead included $T_1(C)$ relaxation times from above the melting temperature (~338 K) of PEO (see Figure 6) as a measure of the amorphous phase mobility well above T_g. The data are in agreement with previous reports on the $T_1(C)$ relaxation of PEO.[36] Clearly, the relaxation rate maximum for uncomplexed PEO is shifted to much lower temperatures in relation to the PEO–salt complex (Figure 6). At about ~300–370 K the relaxation is on the high-temperature side of the $1/T_1(C)$ maximum for PEO, whereas for the polymer–salt complex the relaxation is on the low-temperature side in the same temperature region. This implies a dramatically reduced chain mobility due to the presence of the salt in agreement with the previously discussed line width and $T_{1\rho}(C)$ results.

In Figure 7 we have constructed a relaxation map by plotting the logarithm of the average correlation time vs inverse temperature for the line width maximum, the $1/T_{1\rho}(C)$ maximum and the $1/T_1(C)$ maximum of the present study. For uncomplexed PEO (amorphous phase) of various molecular weights the data are from the literature regarding the α-relaxation, i.e. the molecular motions which, when frozen in, lead to the glass transition (in some of the references the label β is instead used to distinguish from transitions in the crystalline phase). Proton[31,37] and carbon[36] NMR relaxation, dielectric relaxation,[38–40] and T_g[41] data are included in Figure 7. The average correlation time is taken as $\langle\tau\rangle = 1/\omega$, where ω is the peak loss frequency in the case of dielectric relaxation (in some of the references obtained from varied frequency and in some

from varied temperature, which causes a minor spread of the data in Figure 7) or the NMR frequency, as in the present work.

It is interesting to note in Figure 7 that the mobility of uncomplexed PEO shows a strong molecular weight dependence. Normally, the segmental mobility of polymer chains becomes independent of molecular weight once a certain critical degree of polymerization is reached. For example, dynamic light scattering results of amorphous PPO show very little molecular weight dependence for chains longer than ~20 repeat units.[42] In contrast, the glass transition temperature for semicrystalline PEO increases with increasing molecular weight and has a maximum value for a molecular weight of M_n ~5000–6000. Beyond this point the glass transition temperature decreases with increasing molecular weight and becomes constant for molecular weights approximately larger than 10^5 (the glass transition range for PEO is included in Figure 7). Reported data of dynamic glass transitions show qualitatively the same molecular weight dependence. For example, Wobst[37] reports $1/T_\rho$(H) maxima at 286 and 243 K, respectively, for PEO of molecular weight 5000 and 30 000 (Figure 7), in reasonable agreement with the corresponding T_g values.[41] The pronounced molecular weight dependent behavior of PEO has been explained by a changing degree of crystallinity.[41] The highest percent of crystallinity develops for M_n ~5000–6000. For higher molecular weights chain entanglements reduce the crystallinity, which causes less constraints on the amorphous phase and lower values of T_g. In Figure 7 the data of high molecular weight (approximately >10^5) PEO indeed group together, roughly following the free volume WLF temperature dependence of τ determined by Dekmezian et al. from ^{13}C NMR relaxation measurements.[36] Thus, since the PEO–$Ba(ClO_4)_2$ complex of the present study is predominantly amorphous, we may take the data of high molecular weight PEO as a reference for local chain mobility in the amorphous phase.

It is clear from Figure 7 that salt complexation affects the segmental mobility in PEO much more than crystallinity. The time scale of segmental motion is dramatically changed, manifested as a shift of the correlation time curve to higher temperatures for PEO–$Ba(ClO_4)_2$ as compared to uncomplexed PEO. For example, at ~330 K $\langle\tau\rangle$ is about 5 orders of magnitude longer for the PEO–salt complex than for amorphous PEO (high molecular weight). The result is in agreement with the general finding for polyether–salt systems of increased glass transition temperature upon the addition of salt, which has been attributed to the fact that cations act as transient cross-links between the ether oxygens of the polymer chains.[3,4,9,10,13] For PEO–$Ba(ClO_4)_2$ the effect is larger than for previously investigated PPO–$LiClO_4$,[9] PPO–$NaCF_3SO_3$,[10] and PEO–$LiClO_4$[17] and similar to that for PEO–$M(CF_3SO_3)_2$ (where M = Pb or Zn)[16] of comparable salt concentrations, which indicates a very strong interaction for the Ba^{2+} ions with the ether oxygens.

A striking feature in Figure 7 is that $\langle\tau\rangle$ for PEO–$Ba(ClO_4)_2$ is much more sensitive to temperature than that for pure PEO. A similar behavior has previously been reported for PPO–$NaCF_3SO_3$ complexes in comparison with PPO. In the latter study it was suggested that the stronger temperature dependence of structural relaxation times obtained for the PPO–salt complexes is caused by a temperature dependent cross-linking density.[43] At higher temperatures the solvated cations (which interacts with the polymer) tend to form cation–anion pairs and aggregates, thereby decreasing the number of "free" cations available for transient cross-linking. It is possible that ion associations affect the temperature dependence of the correlation time also for PEO–$Ba(ClO_4)_2$. So far, there are no reports on ion association for this system. In this context we also note that it was recently suggested that greater temperature sensitivity of segmental mobility for polymers reflects more intermolecularly cooperative motions (such comparisons are often in the form of Arrhenius plots with the temperature normalized by the respective T_g of each polymer).[44] Thus, chain motion in PEO–$Ba(ClO_4)_2$ may be cooperative in comparison with PEO, which is consistent with a transiently cross-linked structure. It is however not clear whether the interaction between cations and ether oxygens is predominantly intermolecular or intramolecular.

Conclusions

Carbon-13 NMR results of PEO complexed with $Ba(ClO_4)_2$ have clearly shown that the segmental mobility in the amorphous phase is significantly reduced by the solvation of salt. The relatively low PEO chain mobility is due to strong interactions between the ether oxygens and the cations. A temperature increase through T_g decreases the average correlation time much more dramatically for PEO–$Ba(ClO_4)_2$ than for uncomplexed PEO. For a more extensive comparison of the segmental mobility over a wider time window, complementary data from other dynamic techniques would be valuable.

Acknowledgment. We gratefully acknowledge partial support from the Swedish Research Council for Engineering Sciences.

References and Notes

(1) Armand, M. B.; Chabagno, J. M.; Duclot, M. J. Second International Conference on Solid Electrolytes, St. Andrews, 1978.
(2) Armand, M. B. *Annu. Rev. Mater. Sci.* **1986**, *16*, 245.
(3) Ratner, M. A. In *Polymer Electrolyte Reviews*; MacCallum, J. R., Vincent, C. A., Eds.; Elsevier: London and New York, 1987; Vol. 1, Chapter 7, p 173.
(4) Cameron, G. G.; Ingram, M. D. In *Polymer Electrolyte Reviews*; MacCallum, J. R., Vincent, C. A., Eds.; Elsevier: London and New York, 1989; Vol. 2, Chapter 5, p 157.
(5) Chadwick, A. V.; Worboys, M. R. In *Polymer Electrolyte Reviews*; MacCallum, J. R.; Vincent, C. A., Eds.; Elsevier: London and New York, 1987; Vol. 1, Chapter 9, p 275.
(6) Greenbaum, S. G. *Polym. Adv. Technol.* **1993**, *4*, 172.
(7) Wintersgill, M. C.; Fontanella, J. J. In *Polymer Electrolyte Reviews*; MacCallum, J. R., Vincent, C. A., Eds.; Elsevier: London and New York, 1989; Vol. 2, Chapter 2, p 43.
(8) McLin, M. G.; Angell, C. A. *J. Phys. Chem.* **1991**, *95*, 9464.
(9) Sandahl, J.; Börjesson, L.; Stevens, J. R.; Torell, L. M. *Macromolecules* **1990**, *23*, 163.
(10) Sandahl, J.; Schantz, S.; Börjesson, L.; Torell, L. M.; Stevens, J. R. *J. Chem. Phys.* **1989**, *91*, 655.
(11) Schantz, S. *J. Chem. Phys.* **1991**, *94*, 6296.
(12) Kakihana, M.; Schantz, S.; Torell, L. M. *J. Chem. Phys.* **1990**, *92*, 6271.
(13) Bergman, R.; Börjesson, L.; Fytas, G.; Torell, L. M. *J. Non-Cryst. Solids*, in press.
(14) Vachon, C.; Vasco, M.; Perrier, M.; Prud'homme, J. *Macromolecules* **1993**, *26*, 4023.
(15) Spindler, R.; Shriver, D. F. *J. Am. Chem. Soc.* **1988**, *110*, 3036.
(16) Johansson, A.; Wendsjö, A.; Tegenfeldt, J. *Electrochim. Acta* **1992**, *37*, 1487.
(17) Gorecki, W.; Belorizky, E.; Berthier, C.; Donoso, P.; Armand, M. *Electrochim. Acta* **1992**, *37*, 1685.
(18) VanderHart, D. L.; Earl, W. L.; Garroway, A. N. *J. Magn. Reson.* **1981**, *44*, 361.
(19) Rothwell, W. P.; Waugh, J. S. *J. Chem. Phys.* **1981**, *74*, 2721.
(20) VanderHart, D. L.; Garroway, A. N. *J. Chem. Phys.* **1979**, *71*, 2773.
(21) Schaefer, J.; Stejskal, E. O.; Buchdal, R. *Macromolecules* **1977**, *10*, 384.

(22) Allerhand, A.; Doddrell, D.; Komoroski, R. *J. Chem. Phys.* **1971**, *55*, 189.
(23) Jones A. A. High Resolution NMR Spectroscopy of Synthetic Polymers in Bulk. In *Methods in Stereochemical Analysis*; Komoroski, R. A., Ed.; VCH Publishers: New York, 1986; Vol. 7, Chapter 7, p 247.
(24) Lauprêtre, F.; Bokobza, L.; Monnerie, L. *Polymer* **1993**, *34*, 468.
(25) Havriliak, S.; Negami, S. *J. Polym. Sci.* **1966**, *C14*, 99.
(26) Beckman, P. A. *Phys. Rep.* **1988**, *171*, 85.
(27) Maunu, S. L.; Soljamo, K.; Laanterä, M.; Sundholm, F. *Makromol. Chem.* **1994**, *195*, 723.
(28) Campbell, G. C.; Crosby, R. C.; Haw, J. F. *J. Magn. Reson.* **1986**, *69*, 191.
(29) Haw, J. F.; Crook, R. A.; Crosby, R. C. *J. Magn. Reson.* **1986**, *66*, 551.
(30) Torchia, D. A. *J. Magn. Reson.* **1978**, *30*, 613.
(31) Johansson, A.; Tegenfeldt, J. *Macromolecules* **1992**, *25*, 4712.
(32) Dechter, J. J. *J. Polym. Sci., Polym. Lett.* **1985**, *23*, 261.
(33) Cholli, A. L.; Schilling, F. C.; Tonelli, A. E. In *Solid State NMR of Polymers*; Mathias, L. J., Ed.; Plenum Press: New York and London, 1991; Chapter 6, p 117.
(34) Maunu, S. L.; Rinne, H.; Sundholm, F. *Makromol. Chem.*, in press.
(35) Suwelack, D.; Rothwell, W. P.; Waugh, J. S. *J. Chem. Phys.* **1980**, *73*, 2559.
(36) Dekmezian, A.; Axelson, D. E.; Dechter, J. J.; Borah, B.; Mandelkern, L. *J. Polym. Sci. Polym. Phys. Ed.* **1985**, *23*, 367.
(37) Wobst, M. *J. Polym. Sci., Part B: Polym. Phys.* **1988**, *26*, 527.
(38) Fontanella, J. J.; Wintersgill, M. C.; Calame, J. P.; Andeen, C. G. *Solid State Ionics* **1983**, *8*, 333.
(39) Porter, H. P.; Boyd, R. H. *Macromolecules* **1971**, *4*, 589.
(40) Connor, T. M.; Read, B. E.; Williams, E. *J. Appl. Chem.* **1964**, *14*, 74.
(41) Brown, B. D.; de Long, D. J. *Kirk-Othmer Encycl. Chem. Technol.* **1982**, *18*, 616.
(42) Börjesson, L.; Stevens, J. R.; Torell, L. M. *Phys. Scr.* **1987**, *35*, 692.
(43) Torell, L. M.; Jacobsson, P.; Sidebottom, D.; Petersen, G. *Solid State Ionics* **1992**, *53–56*, 1037.
(44) McGrath, K. J.; Ngai, K. L.; Roland, C. M. *Macromolecules* **1992**, *25*, 4911.